

Identification and characterization of hydrothermally altered zones in granite by combining synthetic clay content logs with magnetic mineralogical investigations of drilled rock cuttings

Carola Meller,¹ Agnes Kontny² and Thomas Kohl¹

¹Division of Geothermal Research, Karlsruhe Institute of Technology, D-76131 Karlsruhe, Germany. E-mail: carola.meller@kit.edu

²Division of Structural Geology and Tectonophysics, Karlsruhe Institute of Technology, D-76131 Karlsruhe, Germany

Accepted 2014 July 16. Received 2014 July 15; in original form 2014 February 12

SUMMARY

Clay minerals as products of hydrothermal alteration significantly influence the hydraulic and mechanical properties of crystalline rock. Therefore, the localization and characterization of alteration zones by downhole measurements is a great challenge for the development of geothermal reservoirs. The magnetite bearing granite of the geothermal site in Soultz-sous-Forêts (France) experienced hydrothermal alteration during several tectonic events and clay mineral formation is especially observed in alteration halos around fracture zones. During the formation of clay minerals, magnetite was oxidized into hematite, which significantly reduces the magnetic susceptibility of the granite from ferrimagnetic to mostly paramagnetic values. The aim of this study was to find out if there exists a correlation between synthetic clay content logs (SCCLs) and measurements of magnetic susceptibility on cuttings in the granite in order to characterize their alteration mineralogy. Such a correlation has been proven for core samples of the EPS1 reference well.

SCCLs were created from gamma ray and fracture density logs using a neural network. These logs can localize altered fracture zones in the GPK1–4 wells, where no core material is available. Mass susceptibility from 261 cutting samples of the wells GPK1–GPK4 was compared with the neural network derived synthetic logs. We applied a combination of temperature dependent magnetic susceptibility measurements with optical and electron microscopy, and energy dispersive X-ray spectroscopy to discriminate different stages of alteration.

We found, that also in the granite cuttings an increasing alteration grade is characterized by an advancing oxidation of magnetite into hematite and a reduction of magnetic susceptibility. A challenge to face for the interpretation of magnetic susceptibility data from cuttings material is that extreme alteration grades can also display increased susceptibilities due to the formation of secondary magnetite. Low magnetic susceptibility can also be attributed to primary low magnetite content, if the granite facies changes. In order to interpret magnetic susceptibility from cuttings, contaminations with iron from wear debris of the drilling tools must be eliminated. Provided that the magnetic mineralogy of the granite is known in detail, this method in combination with petrographic investigations is suited to indicate and characterize hydrothermal alteration and the appearance of clay.

Key words: Downhole methods; Rock and mineral magnetism; Hydrothermal systems; Fractures and faults.

1 INTRODUCTION

The experience of more than 10 yr of water circulation and several hydraulic stimulations in the geothermal reservoir of the geothermal power plant in Soultz-sous-Forêts (France) showed, that, in contrast to other enhanced geothermal systems like Basel or Landau (e.g. Catalli *et al.* 2013), the magnitude of seismic events induced by

circulation of fluids is rather low (e.g. Baisch *et al.* 2010). A possible reason for this behaviour is that clay minerals inside fractures can act as lubricants on fault zones and promote aseismic instead of seismic movements as it is observed on the San Andreas Fault (Moore & Lockner 2013). Due to their substantial effect on rock mechanics, such clay rich fracture zones are of major importance for the characterization and engineering of a reservoir. The objective

of our study is the localization of these zones using a correlation between magnetic susceptibility of granite cuttings and the synthetic clay content logs (SCCLs) and proving its reliability.

2 THE SOULTZ-SOUS-FORÊTS SITE

2.1 Geological setting

The geothermal project in Soultz-sous-Forêts at the western border of the Upper Rhine Graben targets a granitic intrusion of Variscan age overlain by 1.4 km Cenozoic and Mesozoic sediments. A porphyritic monzogranite hosts the geothermal reservoir and extends to a depth of ~4800 m forming the main granitic body of the Soultz geothermal system. It is characterized by large kalifeldspar crystals in a matrix of quartz, plagioclase, biotite, amphibole and accessories of magnetite, titanite, apatite, and allanite (e.g. Hooijkaas *et al.* 2006). The reservoir rock has been penetrated by five deviated wells with the deepest well reaching 5260 m measured depth (MD) and a pilot well (EPS1), which has been completely cored to a depth of 2300 m. At 4800 m depth, fine-grained two-mica granite occurs hosting the second geothermal reservoir. It is interpreted as a younger intrusion into the older porphyritic granite and it contains primary muscovite and biotite while kalifeldspar is depleted (Hooijkaas *et al.* 2006). The well trajectories and the different facies are sketched in Fig. 1.

The Soultz intrusions belong to the magnetite series (Ishihara 1977), with primary magnetite as the main carrier of susceptibility. Fresh granite contains ~1 wt-per cent multidomain magnetite with

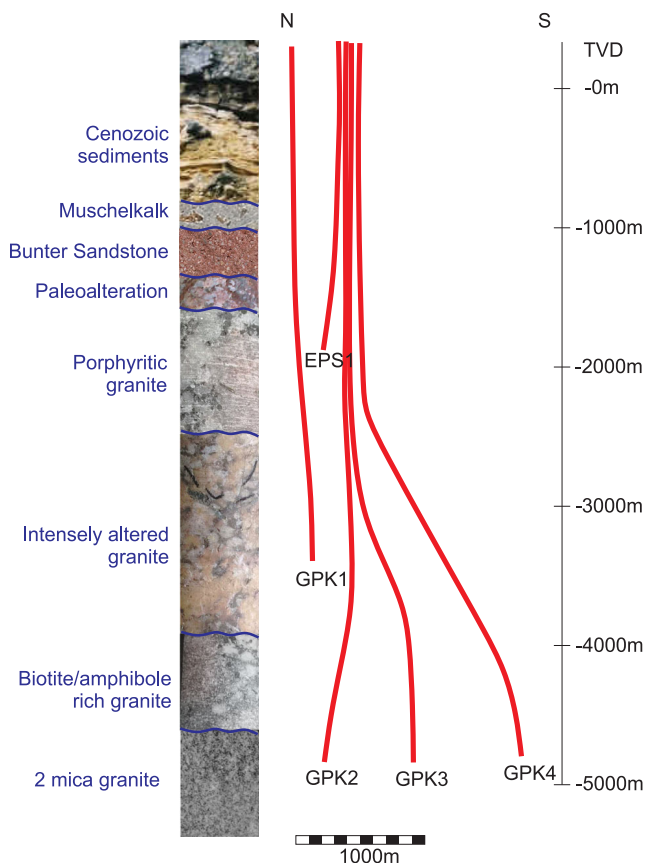


Figure 1. Overview of the trajectories of five deep wells at Soultz and the lithological profile to a depth of ~5000 m true vertical depth (TVD). Sketch is based on borehole trajectory data.

a grain size between 300 and 500 μm . Magnetic susceptibility is between 10 and 80×10^{-3} SI depending on the wt-per cent of magnetite (Just *et al.* 2004).

2.2 The formation of clay minerals during hydrothermal alteration

Due to large-scale wrench tectonics and block rotations during the Cretaceous, large fault zones were formed during the Variscan orogeny (e.g. Edel *et al.* 2013). Such zones provided pathways for fluids, which percolated large areas of the orogenic belt (e.g. Guillou-Frotier *et al.* 2013) and altered the Soultz granite in two major alteration events. The first alteration stage occurred in Middle Carboniferous, when permeable zones formed inside the granite. This pervasive alteration event affected the granitic matrix, but had no influence on the structural properties of the rock (Genter & Traineau 1992). Pervasive alteration is characterized by a transformation of plagioclase and biotite into illite, calcite and chlorite. Just & Kontny (2012) found that during circulation of O_2 -rich fluids, magnetite was partially oxidized into martite in discrete zones near the fluid pathways. In such zones, the grain size of magnetite was reduced and magnetic susceptibility decreased from ferrimagnetic values ($<15 \times 10^{-3}$ SI) to paramagnetic values in the order of 10^{-8} SI. Secondary hematite precipitated from residual fluids.

The second alteration stage took place in Late Carboniferous, when early Variscan fault zones were reactivated. Subsequent circulation of hydrothermal fluids through fractures caused the formation of alteration zones around the fractures as large as several tens of metres. These fracture zones are significantly influencing the structural properties of the granite (Genter & Traineau 1992). The alteration halos are characterized by a central zone, sometimes sealed by quartz, surrounded by brecciated and altered rocks (Genter & Traineau 1992). The alteration intensity varies from fresh (no alteration) to extremely altered facies and is mainly characterized by a transformation of silicates into clay minerals (e.g. Schlicher 2005) and by an increasing amount of secondary clay minerals and carbonates. The main secondary minerals are quartz, calcite, illite, hematite and chlorite. Pyrite and Fe-carbonates were formed and the granite was exhumed to the surface in late Variscan times (Ledésert *et al.* 1996; Fritz *et al.* 2010). In the upper part of the pluton, where meteoric waters infiltrated the paleo-surface, the Fe-carbonates and maghemite ($\gamma\text{-Fe}_2\text{O}_3$) decomposed and secondary fine-grained hematite precipitated (Just & Kontny 2012). Martite pseudo-morphs formed after magnetite grains, whereas the size of the magnetite relics depends on the alteration intensity and on the intensity of stage I alteration. Martite was often fractured and a second hematite generation formed along the cracks. Magnetic susceptibility is mostly below 1×10^{-3} SI and hydrothermally altered wall rocks show the lowest magnetic susceptibility ($0.2\text{--}0.3 \times 10^{-3}$ SI) reflecting the most intense vein alteration. After deposition of the sedimentary cover in Mesozoic times, the infiltration of organic matter from the overlying sedimentary cover reduced martite back into secondary magnetite in the deeper part of the granite (Just 2005).

3 RELEVANCE OF MAGNETIC SUSCEPTIBILITY FOR THE OCCURRENCE OF CLAY MINERALS

Just *et al.* (2004) found that during hydrothermal alteration, which lead to the formation of clay minerals, there was also a

transformation of magnetite (Fe_3O_4) into hematite ($\alpha\text{-Fe}_2\text{O}_3$) (magnetization). This process has previously also been observed elsewhere in granite, basalts and itabirites (e.g. Lagoeiro 1998; Angerer *et al.* 2011; Oliva-Urcia *et al.* 2011). Magnetite oxidation is accompanied by a reduction of magnetic susceptibility (Genter & Traineau 1992).

Core material of the reference well EPS1 provided the unique opportunity to investigate in detail hydrothermal processes and fractures directly on samples. Just *et al.* (2004) compared the bulk magnetic susceptibility log along the EPS1 core of Rummel & König (1991) with the appearance of rock alteration and changes in the magnetic mineralogy. They found, that an increasing alteration grade was accompanied by decreasing magnetic susceptibility.

Meller *et al.* (2014) developed a method to create SCCL on the basis of spectral gamma ray measurements. Such logs provide a semi-quantitative measure of the appearance of clay minerals inside fractures related to hydrothermal alteration. The method to create such logs will be described in the following chapter. According to the results from Just *et al.* (2004), we expected a correlation between the SCCL and magnetic susceptibility of EPS1. Plotting the bulk magnetic susceptibility curve generated after data from Rummel & König (1991) against the SCCL reveals an inverse correlation between the amount of clay and magnetic susceptibility (Fig. 2). This inverse correlation between results from two totally independent methods suggests that magnetic susceptibility can be used as a marker of hydrothermal alteration.

The objective of this work is to create SCCL for the deep Soultz boreholes GPK1-4, where no direct observation of fracture mineralogy is possible due to the lack of core samples. With magnetic mineralogical investigations on cuttings of these wells we wanted to investigate, if the mineralogical changes due to hydrothermal alteration, which have been described on the EPS1 core, can also be observed in the deeper part of the geothermal reservoir.

4 METHODS FOR THE IDENTIFICATION OF VEIN ALTERATION AND ITS MAGNETIC PROPERTIES

The importance of clay as a control to fracture mechanics has been highlighted earlier (Rummel *et al.* 1991; Rummel & Schreiber 1993; Valley & Evans 2003). Clay can be localized by resistivity logs, spontaneous potential logs or sonic logs or it can be identified directly on core material. However, due to low budgeting, boreholes for geothermal applications are generally not cored and only standard (wireline) logs like calliper, image logs and spectral gamma ray are measured. For certain scientific purposes, further logging analyses such as resistivity, spontaneous potential, flow-meter logs, etc. might be conducted. Unfortunately, this is often not the case and if so, these logs are only conducted as spot measurements for selected depth intervals.

In contrast to drill cores, cuttings are obtained from each drilling without additional costs. Most of the structural information about the reservoir is lost in the rock chips of cuttings. Therefore, these rock chips are mainly used for the creation of lithology logs and for geochemical analyses. The loss of structural information, however, plays no role for bulk magnetic susceptibility of the cuttings, as it only depends on the mineralogical content of the sample. With the help of microscopic studies, drilled rock cuttings can provide important additional information about the composition of rocks and chemical processes in a reservoir.

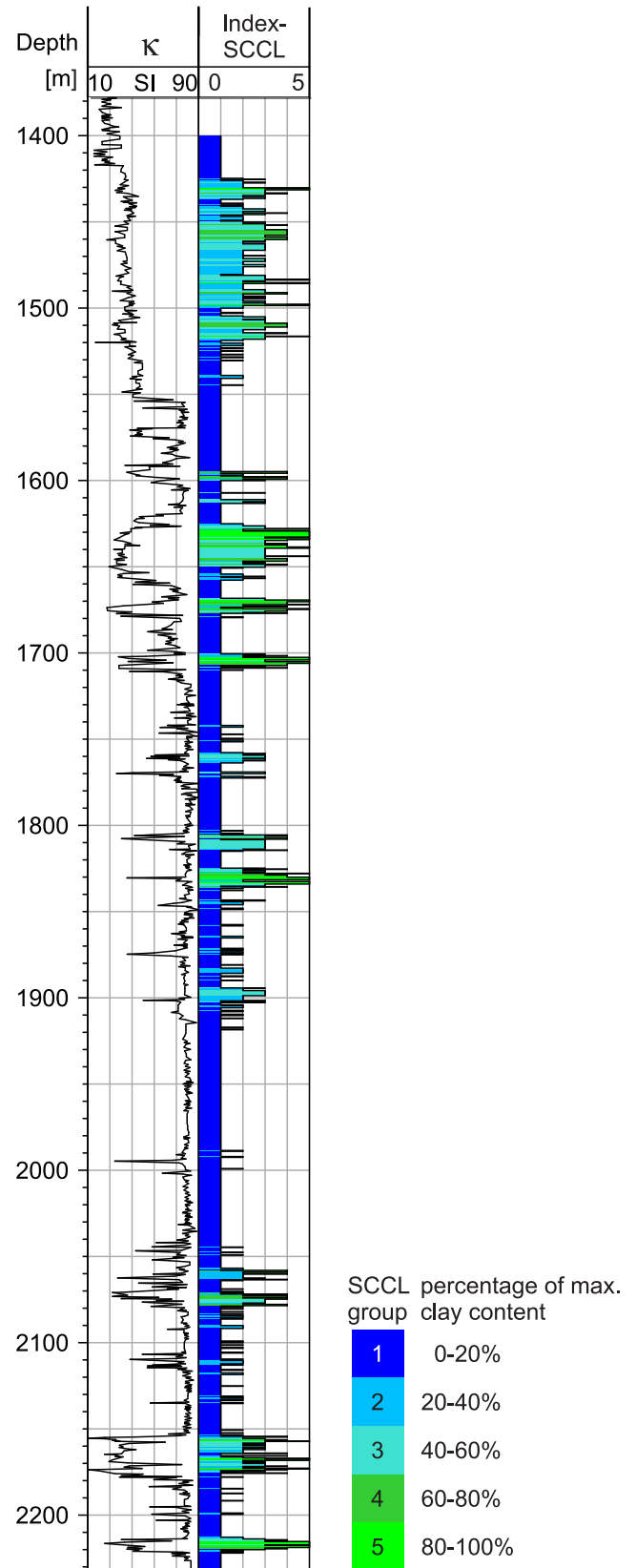


Figure 2. A comparison between the core derived SCCL representing the density of clay-filled fracture along the well with magnetic susceptibility (κ) in 10^{-3} SI of the EPS1 core reveals an excellent correlation between low magnetic susceptibility values and high clay content. Susceptibility data are taken from Rummel & König (1991) and the SCCL is from Meller *et al.* (2014).

Just (2005) verified that hydrothermal alteration is responsible for the transformation of silicates and magnetite oxidation in the granite. This process has also been observed by Pandarinath *et al.* (2013) for the Los Azufres geothermal system in Mexico. The authors found that with increasing depth, hydrothermal alteration increases and the fraction of magnetic minerals decreases. Thus, magnetic susceptibility was found to decrease with depth. Our study focusses on the localization and characterization of hydrothermally altered intervals along the wells GPK1-4 using the temperature-dependence of magnetic susceptibility in combination with microscopic methods on cuttings material.

4.1 Detecting clay from spectral gamma ray logs using a neural network

Meller *et al.* (2014) described a method to find clay bearing fracture zones on the basis of spectral gamma ray and fracture-density logs by applying a neural network on the logging data. They created a reference dataset for the appearance of clay inside fractures on the basis of core data from the pilot well EPS1 at Soultz-sous-Forêts. The reference was used to train the neural network using a Kohonen-algorithm (Kohonen 1984). This algorithm uses a self-organizing map, which is a two-dimensional representation of the multidimensional network. In the training phase, the neural network classifies the input logs in a way that each pattern of log responses is assigned to a node of the neural network. This process is repeated until a certain number of iterations is reached and the network has optimally approximated the input. In the subsequent indexing phase, the network learns how the log responses are correlated with the appearance of clay. For this purpose, the reference clay log is used to group the nodes of the neural network into the predefined SCCL classes. The nodes are distributed into the classes with the closest properties. After this indexing, the network has the knowledge about how clay, fracture density and spectral gamma ray are correlated. This knowledge can be recalled when applying the network on the logs from the remaining wells.

In order to investigate the correlation between alteration intensity, magnetite oxidation, and the formation of clay minerals in the deep wells GPK1, GPK2, GPK3 and GPK4, we applied the network, which was trained on the EPS1 spectral gamma ray and fracture density logs, on the respective logs of the deep Soultz wells.

4.2 Magnetic susceptibility measurements for well characterization

For measurement of magnetic susceptibility and temperature dependence of magnetic susceptibility 261 cutting samples from the following depth intervals of the wells GPK1, GPK3 and GPK4 were selected:

- (i) 147 samples for GPK1 from 1800 to 1829 m, 2594 to 2744 m and 3452 to 3547 m
- (ii) 43 samples for GPK3 from 3296 to 3482 m and 4704 to 4915 m and
- (iii) 71 samples for GPK4 from 3384 to 3542 m and 5030 to 5258 m.

The cuttings are very fine-grained with grain sizes between 0.1 and 1 mm (Fig. 3). GPK2 cuttings were not used due to poor quality.

Bulk magnetic susceptibility was measured with an AGICO KLY-2 Kappabridge with an applied magnetic field of 300 Am^{-1} at a frequency of 920 Hz. Magnetic susceptibility of each

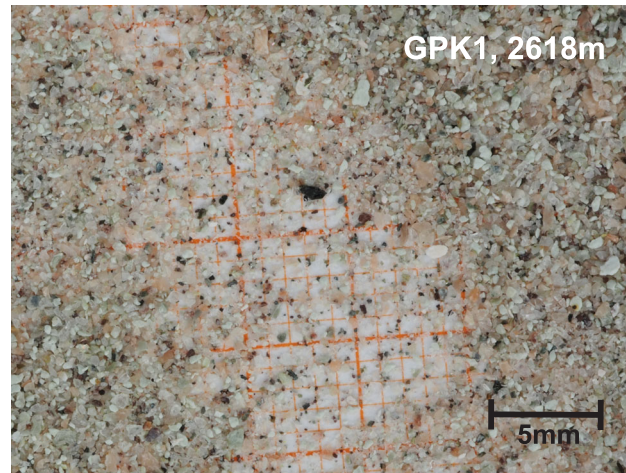


Figure 3. Photo of cuttings from porphyritic granite (GPK1, 2618 m) on millimetre paper.

sample was measured three times and average of these three values is normalized by the sample density.

5 RESULTS

5.1 SCCLs for the wells GPK1-4

The SCCLs of the deeper wells provide a semi-quantitative log of the clay-filled fractures (Fig. 4). They allow discriminating several zones with distinct clay content. This is indicated by five groups of increasing clay content, whereas group 1 represents 0–20 per cent of the maximum density of clay-filled fractures and group 5 represents the highest density (80–100 per cent). The groups are defined in the legends of Figs 2 and 4.

Based on the synthetic logs, we can define several depth intervals with different characteristics from the top to the base of the wells: Interval I, which ends at about 1900 m depth, is characterized by high clay content with SCCL groups 4 and 5. It is followed by interval II, which contains ~ 150 m of low clay (SCCL 1 and 2) with a central structure with SCCL 4 and 5 indicating a clay-rich interval at about 2100 m. This interval can be observed in all four wells. In GPK1 and GPK2 (Figs 4a and b), interval III contains a succession of small intervals with changing contents of clay-filled fractures. In interval III of the wells GPK3 and GPK4 (Figs 4c and d) the SCCL is generally higher and it can be subdivided into two subintervals IIIa and IIIb. IIIa contains several broad and clay-rich structures alternating with intervals of low SCCL (little clay). Interval IIIb has high SCCL values in GPK3, but smaller SCCL values in GPK4. Interval IV is characterized by low SCCL in GPK2 and 3, whereas in GPK2 fracture information is missing in this depth and the SCCL log might not be correct. In GPK1 and GPK4, there are broad intervals of intermediate SCCL (groups 2 and 3) alternating with thick intervals without or with very little clay (SCCL group 1 and 2). The deepest interval V beginning at a depth of ~ 4600 m again shows an increased density of clay-filled fractures, which might be due to the transition of porphyritic granite to the fine-grained two-mica granite.

Resuming, the highest SCCL is expected in the upper parts of the wells (interval I) and around the structure at ~ 2100 m in all wells. Furthermore, clay-rich zones occur in GPK1 around 2700, 2900 and 3300–3500 m. In GPK2, high SCCL values indicate high clay content between 4600 and 4800 m. GPK3 has several clay-rich

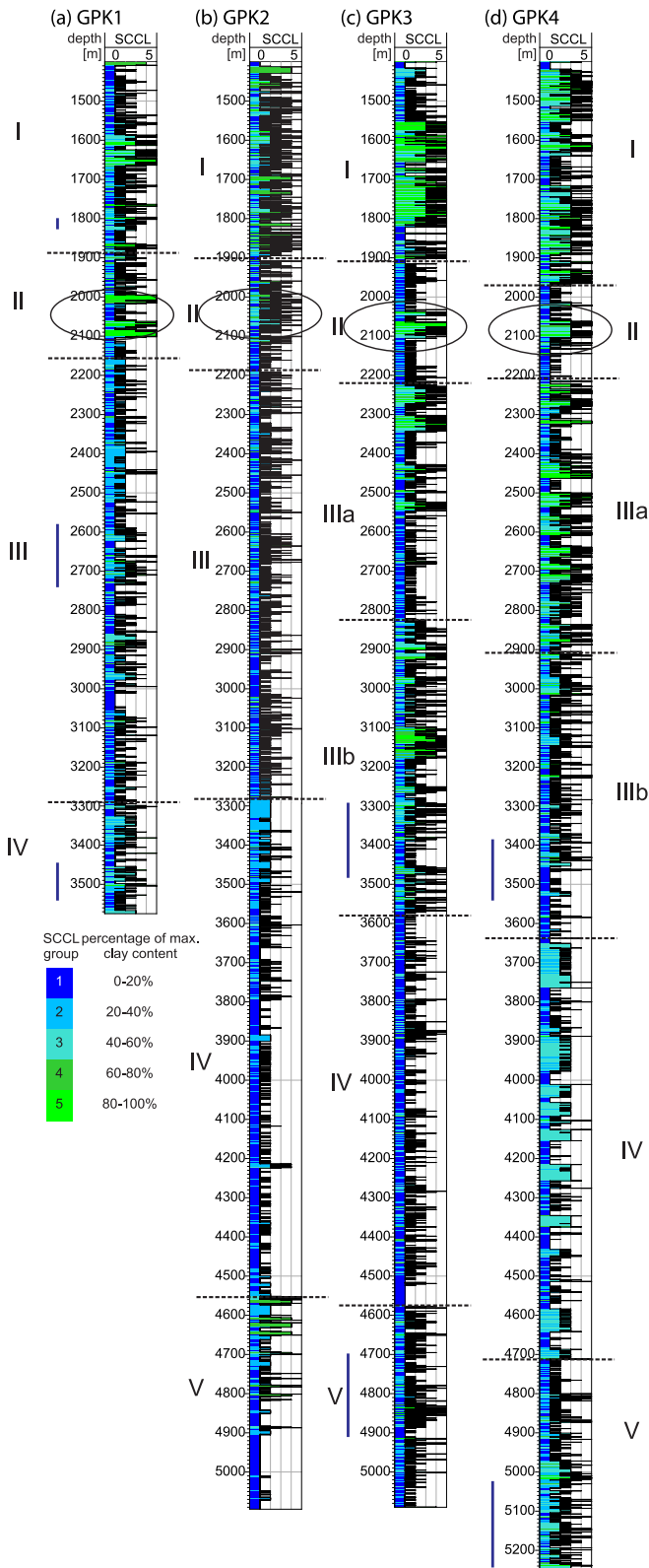


Figure 4. SCCLs for the wells GPK1-GPK4 created by the neural network application. The colours represent the different groups of increasing density of clay-filled fractures as explained by the legend. The blue lines beside the logs indicate the depth intervals, for which cuttings were available. The logs are subdivided into four respectively five depth intervals I–IV or V, which are similar in each well. The black ellipse in zone II highlights a clay-rich structure, which can be seen in each well.

intervals between 2800 and 3600 m and below 4600 m. GPK4 is the well with the highest SCCL, especially in the intervals IIIa, IV and V.

5.2 Magnetic susceptibility of cuttings

Large variations of mass magnetic susceptibility have been measured for the three wells, ranging from $\chi = 0.16$ to $7.35 \times 10^{-3} \text{ m}^3 \text{ kg}^{-1}$ for GPK1, $\chi = 0.24$ to $8.92 \times 10^{-3} \text{ m}^3 \text{ kg}^{-1}$ for GPK3 and $\chi = 1.59$ to $17.91 \times 10^{-3} \text{ m}^3 \text{ kg}^{-1}$ for GPK4. In the following, the symbol χ indicates mass susceptibility in $10^{-3} \text{ m}^3 \text{ kg}^{-1}$, whereas κ in Fig. 2 is bulk susceptibility in SI. From the described previous data we expected higher χ in fresh granite than in the altered granite. Fig. 5 shows exemplary results for different reservoir depths with increasing depth from GPK1 to GPK4. The GPK1 interval around 1500 m is neglected as this interval is characterized by high paleo-alteration intensity. This alteration is not of interest for this study. A comparison between the measured χ and the respective lithology (Fig. 5) indicate that the strong correlation between susceptibility and SCCL seen in Fig. 2 is not always apparent. However, there is a tendency towards higher χ in the porphyritic granite than in altered facies (Figs 5a and b).

The SCCL can better explain intervals of low χ than the lithology log. In the depth interval 2625–2660 m of GPK1, the litholog indicates fresh porphyritic granite. χ is only high between 2625 and 2640 m followed by a slight decrease. In contrast to the lithology log, the SCCL log indicates the appearance of clay-filled fractures between 2640 and 2660 m, which are a sign for alteration in this interval. This is in accordance with low magnetic susceptibility. Poor correlation between χ and SCCL can be found, for example, in the extremely altered facies between 3490 and 3500 m in GPK1 (Fig. 5b) or in the fresh porphyritic granite between 4780 and 4810 m in GPK3 (Fig. 5c). In alternating sequences in the order of few metres, there is poor correlation between alteration and χ . We assume that this is a result of the large sampling interval, which is in the order of the thickness of lithological units. An important observation is that the transition between porphyritic and two mica granite correlates with a decrease of χ (Fig. 5c). The two mica granite is characterized by lower magnetite content than the porphyritic granite.

With a statistical analysis of SCCL versus magnetic susceptibility we further investigated the correlation between magnetic susceptibility logs and the SCCL logs.

The cross-plot of SCCL group number versus mass susceptibility (Fig. 6) reveals that χ is inversely correlated with the clay content indicated by the SCCL. The mean mass magnetic susceptibilities ($\bar{\chi}$) and their respective standard deviation (σ^2) measured for the five SCCL groups are:

- Group 1: $\bar{\chi} = 3.5$ ($\sigma^2 = 4.97$)
- Group 2: $\bar{\chi} = 3.01$ ($\sigma^2 = 4.62$)
- Group 3: $\bar{\chi} = 2.24$ ($\sigma^2 = 1.96$)
- Group 4: $\bar{\chi} = 1.61$ ($\sigma^2 = 1.54$)
- Group 5: $\bar{\chi} = 0.42$ ($\sigma^2 = 0.28$)

$\bar{\chi}$ is lower for higher clay content, which is in agreement with the results of the measurements done by Just *et al.* (2004). Although the mean values indicate decreasing susceptibility with increasing clay content, there is a large scattering of χ in each SCCL group (Fig. 7a), which is also reflected by the large standard deviation of $\bar{\chi}$ (Fig. 6). According to the observation in EPS1 that magnetic susceptibility decreases with increasing clay content, we would expect the lowest

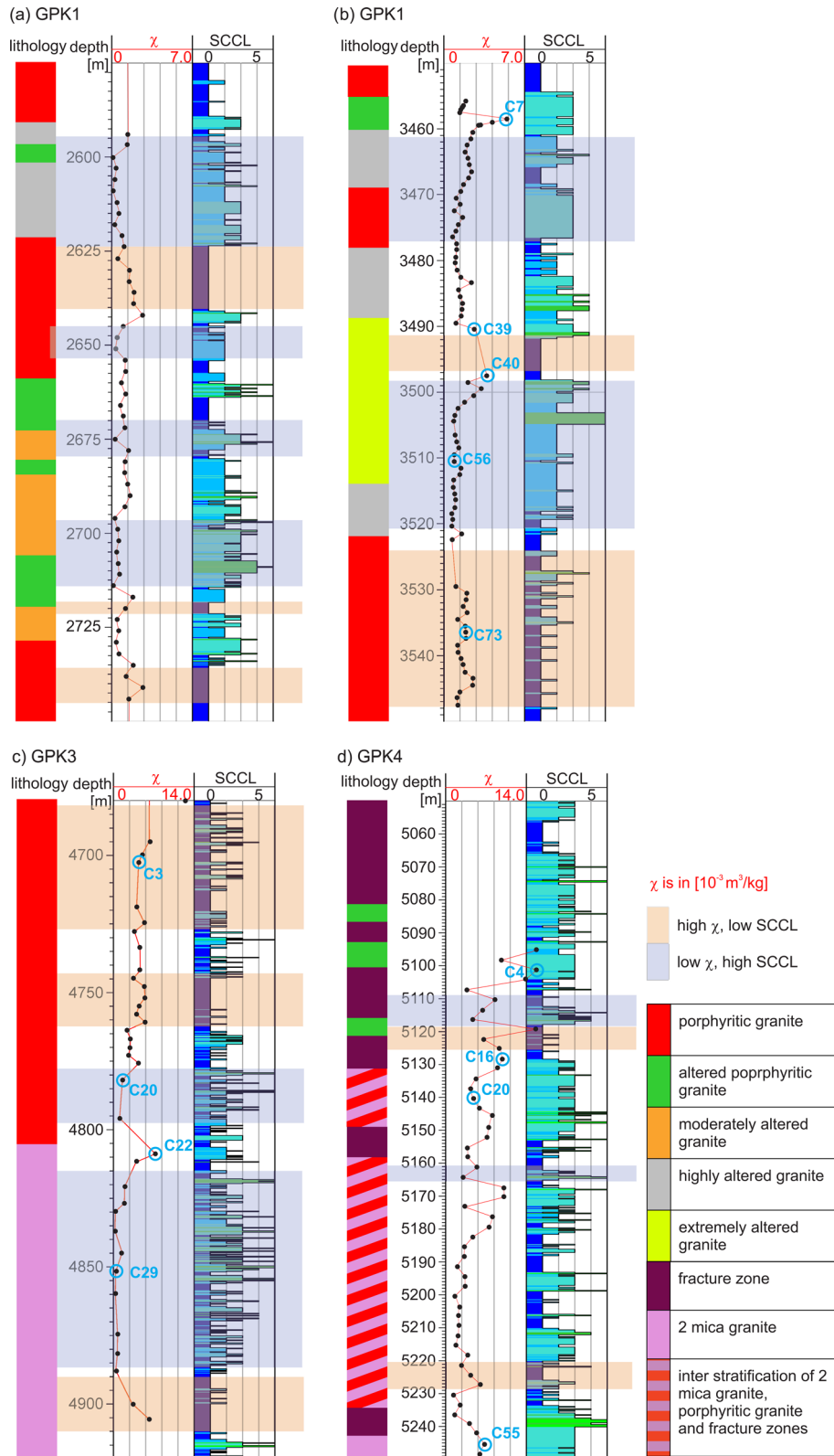


Figure 5. GPK1, GPK3 and GPK4 susceptibility logs derived from measurements of the mass susceptibility of cuttings. Shown is a comparison between SCCL and mass susceptibility of cuttings for certain depth intervals of GPK1, GPK3 and GPK4. The coloured bars indicate where low magnetic susceptibility correlates with high clay content (blue) and vice versa (brown). The simplified lithology is created after the litholog derived from cuttings examination by Genter & Traineau (1993) for GPK1, Dezayas *et al.* (2003) for GPK3 and Dezayas *et al.* (2005) for GPK4. The colours are explained in the legend. Blue circles indicate the selected samples for κ -T measurements and thin section analyses.

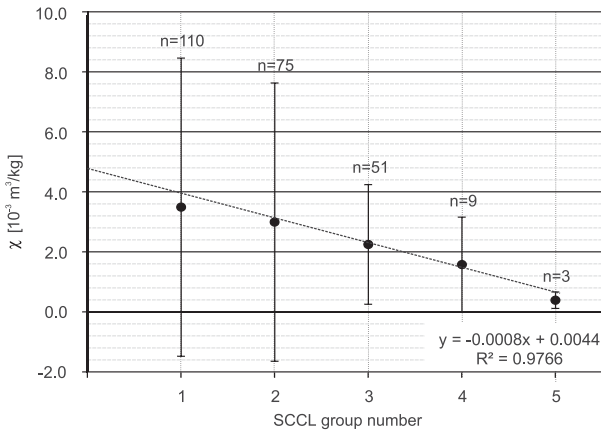


Figure 6. Synthetic clay content log groups versus mass susceptibility of cuttings. With increasing group number, that is higher clay content, mass magnetic susceptibility (χ) is lower. Circles represent the mean values of measured magnetic susceptibility and bars indicate the standard deviations. The dashed line is the regression line. The equation of the regression line and the R^2 value are given in the lower right-hand corner of the diagram.

χ for the SCCL groups 4 and 5, yet low χ is measured for all SCCL groups. This may be due to the varying amount of magnetite present in the samples, and the diluting effect on cuttings material by large phenocrysts of feldspar with diamagnetic to paramagnetic χ values. Alternatively, the blending of sample material from different depth intervals may dilute the χ intensity. As a result, minerals from depth intervals with different alteration grades and different SCCLs can

be mixed, which means that the SCCL assigned to a sample might not be representative for that interval. For GPK4, for example, the sampling interval was between three and 24 m (Dezayes *et al.* 2005). In GPK3, the maximum distance between two samples was 16 m. This might be the reason, why the largest scattering of χ versus SCCL can be observed in GPK3 and GPK4 (Figs 7c and d), whereas scattering is lowest in GPK1 (Fig. 7d). Here, the sampling interval was 1 m, the highest number of samples available. In the GPK1 well, a clear tendency towards higher χ was found in the fresh granite and towards lower values in the clay-rich sections (Fig. 5). Although the scattering of χ is high, we measured the highest χ only in fresh lithology (SCCL groups 1 and 2).

For the well GPK4, the minimum χ in each SCCL group is considerably higher than for the GPK1 samples, but there is no clear indication from lithology explaining the different behaviours. We assume that magnetic susceptibility is increased due to contamination of the cuttings by wear debris from the drill bit or other drilling tools. This aspect has been further investigated by microscopic examination of the samples.

6 CHARACTERIZATION OF HYDROTHERMAL ALTERATION BY MAGNETIC MINERALOGICAL INVESTIGATIONS OF CUTTINGS

The excellent correlation between decreasing χ and the appearance of clay, which has been demonstrated on the EPS1 core (Fig. 2), has not always been observed in the magnetic susceptibility

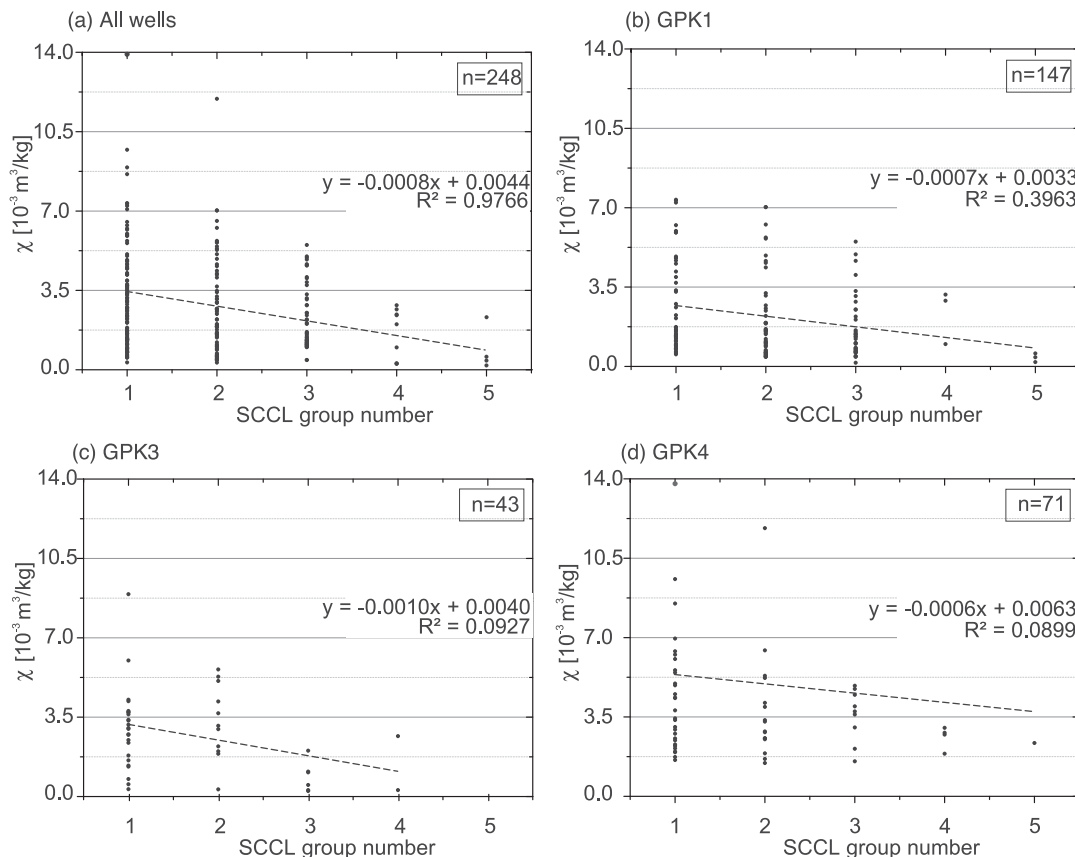


Figure 7. Measured susceptibility values for the different SCCL groups for all wells (a) and separated for GPK1 (b), GPK3 (c) and GPK4 (d). The dashed line is the regression line with the respective equations and R^2 value given in the diagram. For GPK4 four χ values of SCCL1 and SCCL2 are above ~ 14 . These samples are not plotted here and are excluded for the regression calculation.

measurements of cuttings. Therefore, a more detailed understanding of the magnetic mineralogy of cutting samples is necessary to correctly interpret the results. The following section summarizes the main aspects of our magnetic mineralogical investigations. These results are compared to earlier investigations on EPS1 core material by Just *et al.* (2004) and Just & Kontny (2012).

6.1 Mineralogical and magnetic methods

Magnetic mineral assemblages in fresh and altered granite cuttings were studied from samples with very low and very high susceptibility, respectively (blue circles in Fig. 5). Twelve samples were selected for thin section investigations under reflected and transmitted light using a Leitz Orthoplan optical microscope. Two samples were additionally investigated by electron microscopy (Quanta FEG 650 from FEI, with an acceleration voltage of 15 kV) and with energy dispersive X-ray spectroscopy (EDX) using a Quantax 400 with an XFlash-Detector, in combination with the software Esprit 1.9 from Bruker AXS Microanalysis GmbH. In order to explain the behaviour of samples with intermediate to high susceptibility but different degrees of alteration in the SCCL, the altered sample GPK1-C40 and the fresh sample GPK1-C73 from the porphyritic granite were selected. Our goals were to identify and to compare their carriers of magnetic susceptibility and the mineral assemblage.

Magnetic susceptibility as a function of temperature (κ - T curves) was measured for 16 samples (~ 0.2 g) in order to determine Curie points and to characterize mineral transformations, which is useful for the identification of magnetic minerals. κ - T curves were measured with a KLY-4S Kappabridge applying a magnetic field of 300 Am^{-1} and a frequency of 875 Hz. The sample was first heated from -192°C to room temperature (low-temperature run) with a heating rate of approximately 4°C min^{-1} . Afterwards, the sample was measured from ambient temperature to 700°C and cooled back to room temperature with a heating rate of $10^\circ\text{C min}^{-1}$. The measurements were conducted in an Argon atmosphere with a flow rate of 100 ml min^{-1} to minimize mineral reactions with atmospheric oxygen during heating. The raw data were corrected for the empty furnace and normalized to χ at room temperature.

6.2 Results of magnetic mineralogical investigations

6.2.1 Microscopic identification of mineral phases

Two distinct granite facies occur in the granitic body of the Soultz geothermal system; the porphyritic granite and the two-mica granite (Fig. 5). The main focus of our cuttings investigation involved the porphyritic granite because alteration stages are better defined in this facies. The porphyritic granite contains large phenocrysts of K-feldspar and a coarse grained matrix of quartz, biotite, and plagioclase. Accessory phases are mainly zircon, titanite, sometimes with inclusions of lamellar hemo-ilmenite grains and pyrite (Figs 8a and b), and magnetite.

Thin sections of cuttings of two-mica granite from the deeper part of the GPK4 well look different from those of the GPK1 and GPK3 wells. The occurrence of cross-hatched microcline and myrmekite is typical for the two-mica granite facies and has already been described by Dezayes *et al.* (2005). Microcline and myrmekite can be seen in thin sections as well as muscovite associated with biotite. In the two mica granite, we have also identified magnetite as the main magnetic mineral albeit its abundance seems to be less than

in the porphyritic granite. However, we were not able to quantify the different contents of magnetite in the two granite facies as their distribution is heterogeneous.

Cutting samples from the altered granite are characterized by a higher amount of hematite than magnetite. Both minerals are always intergrown, indicating a replacement relationship (Fig. 9a). It is not clear if magnetite replaces hematite or if magnetite is transformed into hematite in these grains. Just & Kontny (2012) also observed an intergrowth of magnetite and hematite in thin sections of granite from stage I alteration (see fig. 3d in Just & Kontny 2012). In addition to a higher amount of hematite, we observed iron-bearing carbonates in the more altered samples (Figs 9b and c).

A frequently observed paragenesis in altered samples is that of allanite, rutile, apatite and titanite with iron oxides (Figs 9e and f). Goethite and hematite occur as alteration seams around the fractured cuttings. This alteration appears not to be a product of hydrothermal alteration, but rather a secondary effect due to humidity inside the stored samples. We recognized, that iron-oxide alteration seams are more pronounced in the samples of GPK1 than in those of GPK3 and GPK4. GPK1 was drilled in 1992 and therefore these samples are older than the samples from GPK3 and GPK4 that were drilled in 2002 and 2003/2004, respectively. This means, they have been exposed longer to atmospheric oxygen and moisture. Therefore, we attribute the more pronounced oxidation to the long storage time of the GPK1 samples. Such an alteration due to storage has also been observed around iron flakes, which occur as contaminations in the cuttings (Fig. 9g). The EDX spectrum of the iron flake showed iron, oxygen, manganese, chromium and silica (Fig. 9h), which probably reflect the composition of the material of the drilling tool. The oxidation rim around the flakes only showed iron and oxygen.

6.2.2 κ - T curves

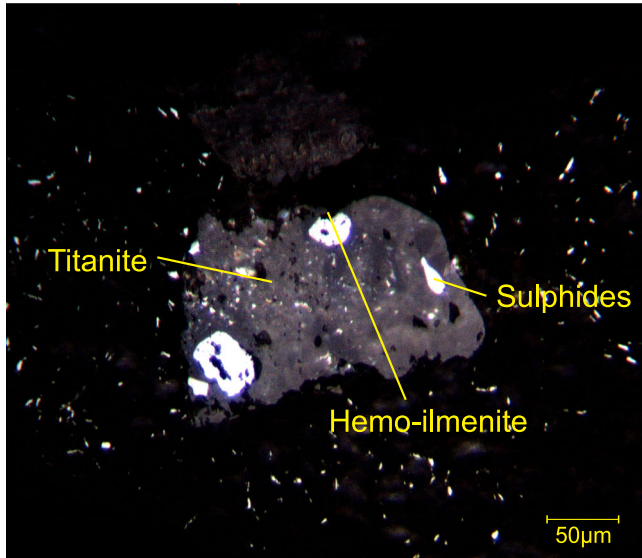
Fig. 10 shows typical κ - T curves of fresh and altered porphyritic and two-mica granite from the GPK1-4 wells. In all samples, magnetite was identified as the main carrier of magnetic susceptibility, which is indicated by the occurrence of the Verwey transition (T_V) at 120 K (-153°C) and a Curie temperature at $\sim 580^\circ\text{C}$.

Fresh and altered granite cuttings of well GPK3 and four are all contaminated by iron debris (Figs 10a, b and d) indicated by the magnetic susceptibility behaviour between 600 and 700°C where magnetic susceptibility does not reach zero. Even the GPK1 cuttings stored for the last 20 yr occasionally contain iron flakes (Figs 9g and h). These iron flakes were, however, no longer recognized in κ - T curves of GPK1 samples (Fig. 10c), which indicates their oxidation (formation of rust) and therefore their rare survival over this time period.

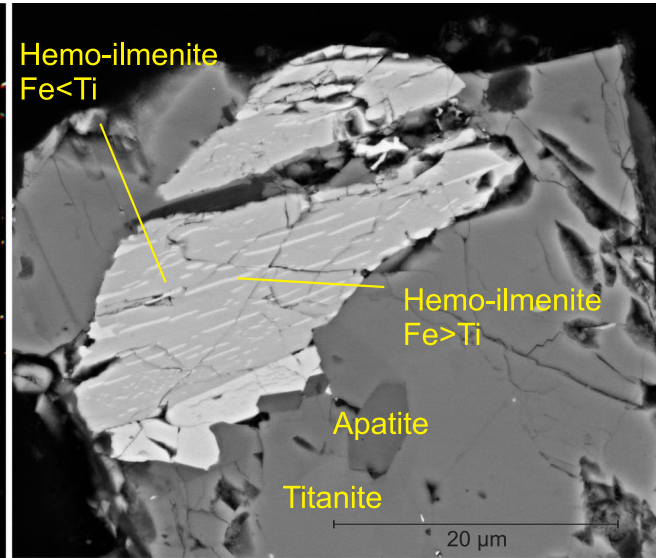
In the altered sample of the porphyritic granite (Fig. 10c), a transformation above 400°C into a ferrimagnetic phase has been observed. This feature can be related to iron-bearing carbonates, which transform at this temperature into a ferrimagnetic spinel phase (Just & Kontny 2012), and which is also in agreement with our microscopic observations (Figs 9b-d). This interpretation is supported by the cooling curve, which only shows magnetite and a ferrimagnetic phase with a Curie point at 499°C (inflection point method, Tauxe 1998) and the features from the heating curves are destroyed.

The difference in the reversibility of the κ - T curves indicates that a degree of alteration occurred during the heating experiment. In the cooling run of the GPK1 samples, susceptibility is considerably higher than in the heating run. This indicates the formation of

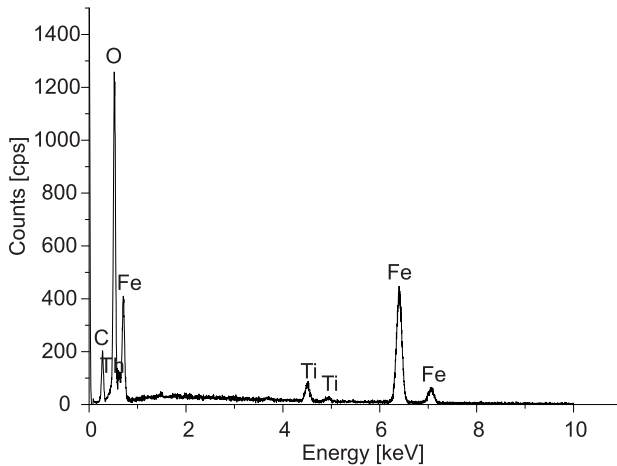
(a) GPK1-C73, reflected light



(b) GPK1 C73, BSE image



(c) EDX spectrum haemo-ilmenite Fe>Ti



(d) EDX spectrum haemo-ilmenite Fe<Ti

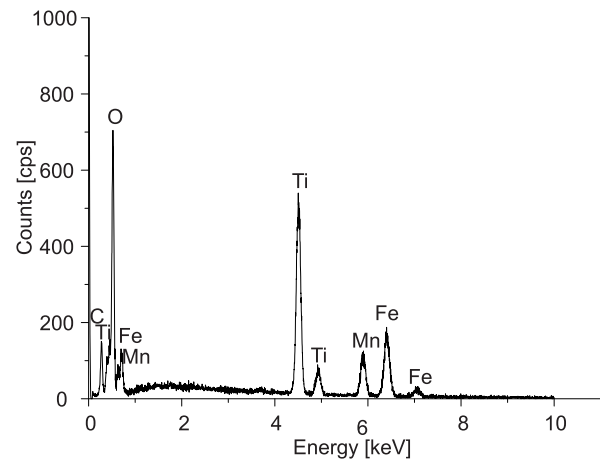


Figure 8. Microscopy of the sample GPK1-C73 (fresh granite). (a) is in reflected light, (b) is a back-scattered electron photograph, (c) and (d) are EDX spectra of hemo-ilmenites with different titanium contents.

new ferrimagnetic mineral phases (e.g. magnetite from hematite or secondary Fe-bearing carbonates) during the heating run. The curves confirm the observation by Just & Kontny (2012), who found that more pronounced stage II alteration in the sample is reflected by less reversibility of the susceptibility curve. They defined an alteration index (AI) similar to that of Hrouda (2003) as a measure for the irreversibility of κ - T curves, calculated according to the formula $AI = \kappa_{CTroom} - \kappa_{HTroom}$, where κ_{CTroom} and κ_{HTroom} are the normalized susceptibility of the cooling, respectively heating run at room temperature.

For less altered samples, AI is <1 , whereas more altered samples have $AI >1$ with the highest values measured for stage II alteration (maximum of 4.8). Samples of GPK4 show a negative alteration index, which indicates the decomposition of magnetite or a transformation of the iron chips during heating. However, this behaviour is not observed in the κ - T curve of the separated iron chips (Fig. 11), which have an alteration index of 0.04. This suggests that the iron chips increase the absolute value of magnetic susceptibility of the samples, but do not affect the alteration index.

Although identified by its red internal reflections in thin sections, hematite was not seen directly in κ - T curves. No Morin transition of hematite at 263 K (-10°C) or Néel temperature at 675°C was observed. We assume that magnetite masks the Morin transition of hematite, whose susceptibility is three orders of magnitude weaker than that of magnetite. The missing Néel temperature and the increase of magnetite content during the heating experiment indicate that hematite is transformed into magnetite. Therefore, higher alteration indexes in the altered granite samples are mainly related to the transformation of hematite and iron-bearing carbonates into magnetite.

Some fresh and altered cutting samples of all wells, but most pronounced in GPK1 (Figs 12a and c), show a conspicuous increase in magnetic susceptibility at about 250°C forming a peak at about 300°C , which is followed by a decrease. Between about 400 and 580°C magnetic susceptibility is higher than below 250°C indicating that a phase with higher magnetic susceptibility must have formed. This phase is not stable during the heating procedure and transforms presumably into magnetite. An increase in

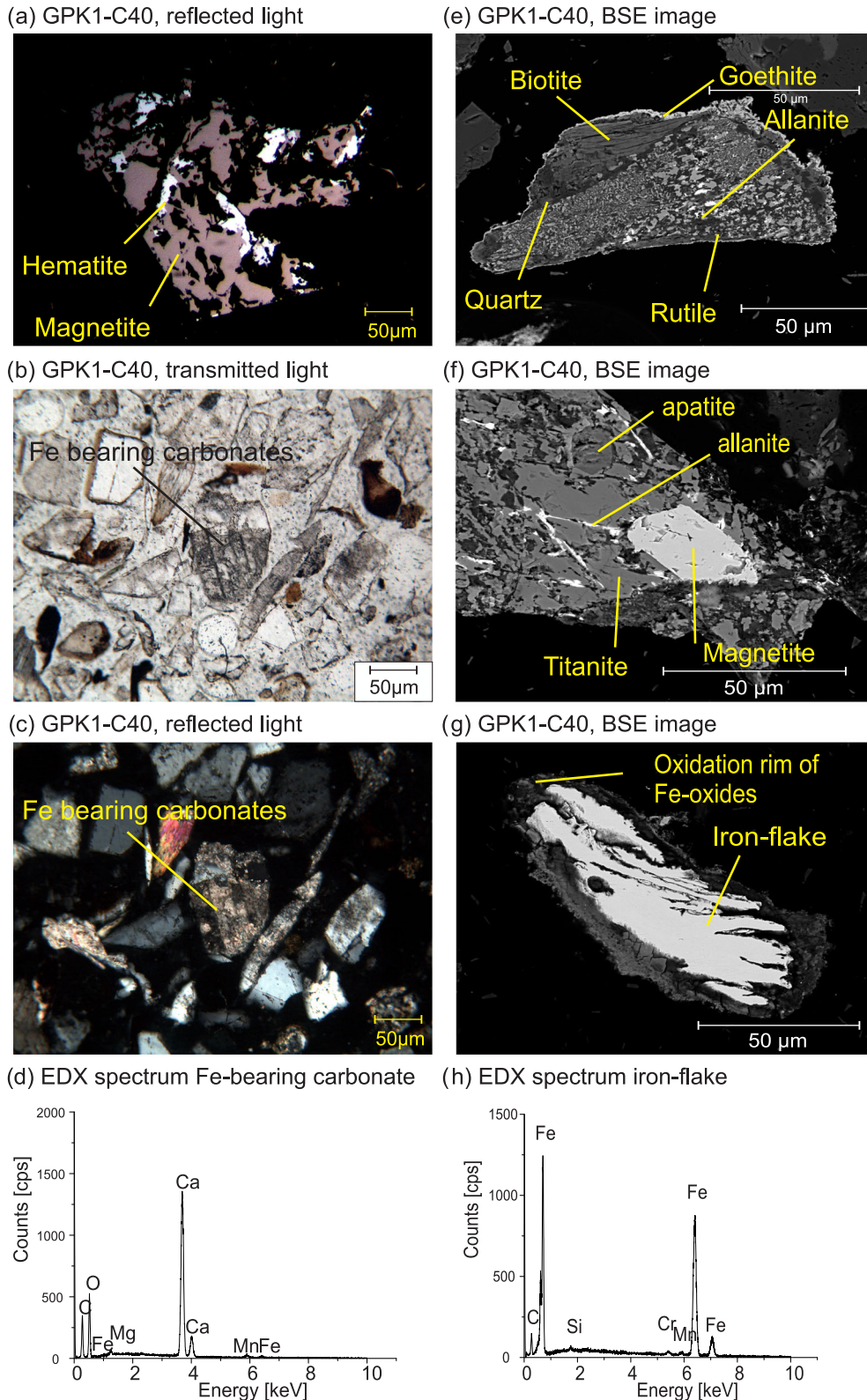


Figure 9. Microscopy, BSE images and EDX spectra of some minerals in the sample GPK1-C40 (altered granite).

magnetic susceptibility is for example observed at the λ -transition of minerals, which is a change in the magnetic state by a rearrangement of vacancies. Although the strong increase in susceptibility at 250 °C resembles the one observed for the λ -transition of hexagonal pyrrhotite (e.g. Kontny *et al.* 2000), where the magnetic state

of the mineral changes from antiferromagnetic to ferrimagnetic, and the Curie temperature at about 350 °C might be indicative for ferrimagnetic iron sulphides like smythite or greigite (Dunlop & Özdemir 1997), we have microscopically identified pyrite as the only occurring iron sulphide. Samples with the conspicuous peak

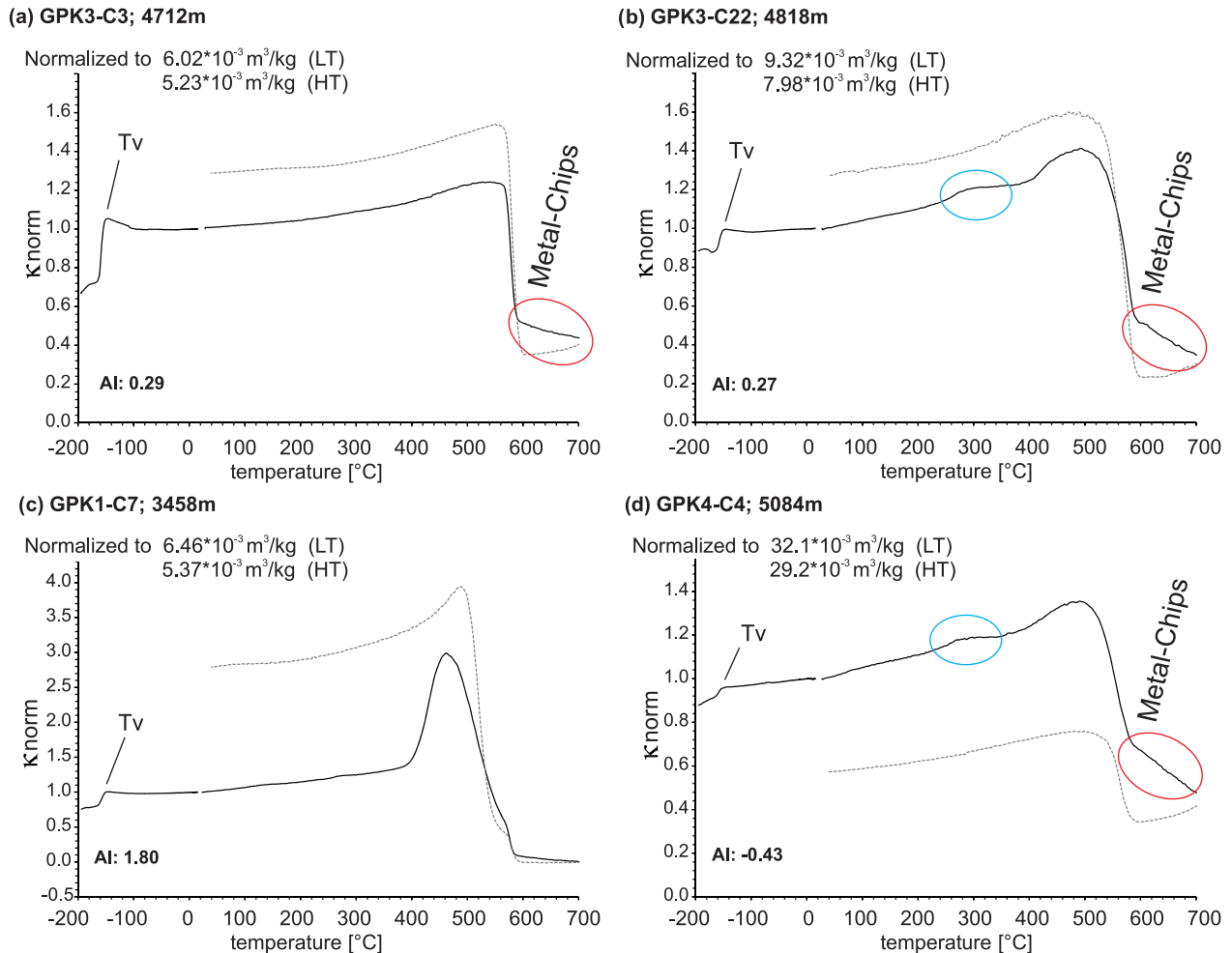


Figure 10. κ - T curves for the samples (a) GPK3-C3 (porphyritic granite), (b) GPK3-C22 (two-mica granite), (c) GPK1-C7 (altered porphyritic granite) and (d) GPK4-C4 (altered two-mica granite). Susceptibility is normalized to the susceptibility at room temperature for the low-temperature (LT) and high temperature run (HT) as indicated in the upper left-hand corner of the graphs. The black curves show the heating run and the grey curves the cooling run, respectively. The alteration index (AI) is given for each curve.

at about 300 °C also do not show a pronounced field-dependence of magnetic susceptibility (Figs 12b and c), which would be a clear indication of ferrimagnetic pyrrhotite (e.g. Hrouda 2003).

A similar but not equivalent bump in κ - T curves was observed by Petronis *et al.* (2011) in the Western Granite from NW Scotland and is actually widespread for magnetite-bearing rocks (Hrouda 2003). This feature is in general attributed to maghemite, an oxidation product of magnetite.

Because we clearly see that a new phase with higher magnetic susceptibility has formed at 250 °C (higher magnetic susceptibility level between 400 and 580 °C), we suspect that we see a two-stage phase transformation of a phase with lower magnetic susceptibility to a strong ferrimagnetic phase (or we see a Hopkinson peak of a ferrimagnetic phase with small grain sizes) and then to magnetite. We suspect that the peak might be attributed to the formation of maghemite from the oxidation products of the iron chips, which is transformed in the course of further heating to magnetite. Maghemite formation is often observed during heating of iron oxides like goethite or hematite (e.g. Cornell & Schwertmann 2003). This interpretation would be in agreement with the observation that this behaviour is most pronounced in cutting samples from the GPK1 well, in which iron flakes are most oxidized.

In order to find an evidence for this hypothesis we selected some iron chips from the sample GPK1-C40 (see Fig. 12a) and measured a κ - T curve (Fig. 11). Magnetic susceptibility increases continuously during heating of the iron chips, but below 300 °C the gradient of the curve becomes steeper reaching a maximum at around 260 °C and forming a peak at 280 °C. This is probably the same peak, which we observed in the κ - T curves of the cutting samples. Further heating clearly indicates the formation of magnetite, which is a major phase of the iron flakes. We relate this behaviour to the oxidation seams around the iron chips and take it as evidence for our hypothesis that the 300 °C peak in our samples is mainly related to oxidation products of the iron flakes.

7 DISCUSSION

7.1 SCCL logs from spectral gamma ray data

The application of the neural network method (Meller *et al.* 2014) makes it possible to find altered and clay rich zones along the geothermal wells. In general, the logs allow discriminating between five different intervals of high and low clay content, respectively.

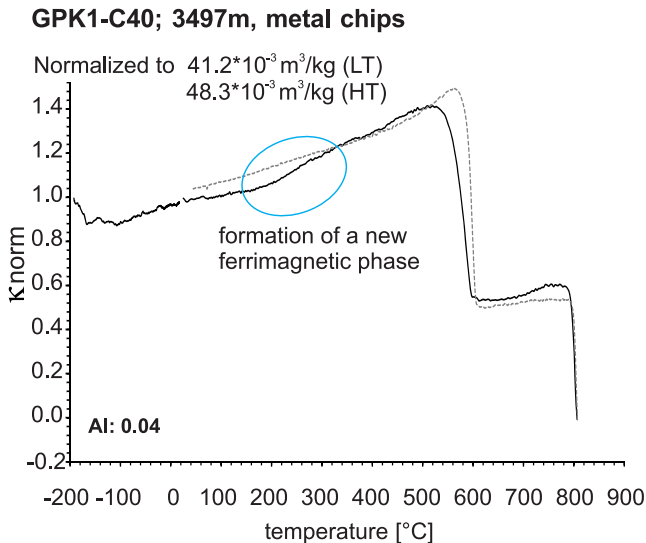


Figure 11. κ - T curve of iron chips separated from the sample GPK1-C40. The curve shows the formation of a new ferromagnetic phase (probably magnetite) during heating. The newly formed magnetite is indicated by its Curie-temperature. The sample is demagnetized at 800 °C.

The logs show a high content of clay-filled fractures in the upper part of all four deep wells. In the deeper parts of the reservoir, the patterns are different between the boreholes, which might be due to the fact that the upper parts of the wells are very close to each other, whereas below 3000 m the wells are increasingly deviated from each other. The change in lithology is not clearly visible in the SCCL logs, but the transition from intensely altered facies to two-mica and amphibole rich granite at ~3500 m and the transition to the fine-grained two-mica granite at ~4600 m are reflected by a change in clay content and in the pattern of clay appearance.

Several structures can be identified, which might indicate fracture or alteration zones, and have not been taken into account in previous studies. This is for example a structure at 2100 m MD, which can be seen in all four deep wells and in EPS1. A large fracture zone has been identified in GPK3 and EPS1 (Genter & Traineau 1995; Dezayes *et al.* 2000), but not for the remaining wells. Such zones are related to vein alteration and the high clay content can weaken the granitic rock. The identification of these potentially weak zones is important as they most probably behave different than the intact or unaltered rock mass.

Compared to previous petrographic approaches for the localization of altered zones, this SCCL method is independent from cutting losses or other drilling-related effects, which can lower the quality of the cutting material. It is based on standard logging techniques and provides the possibility to obtain complete synthetic logs in a rather short time.

7.2 Characterization of rock alteration by magnetic mineralogical investigations

Magnetite was found in all samples from which we measured κ - T curves independent of granite type and degree of alteration, although the proportion is small in the altered samples. The strong decrease of magnetic susceptibility in the altered samples can be related to the oxidation of magnetite to hematite as already stated by Just *et al.* (2004) and Just & Kontny (2012). According to these earlier studies on the EPS1 cores, a significant decrease of magnetic susceptibility occurs in stage II altered granite, which is restricted

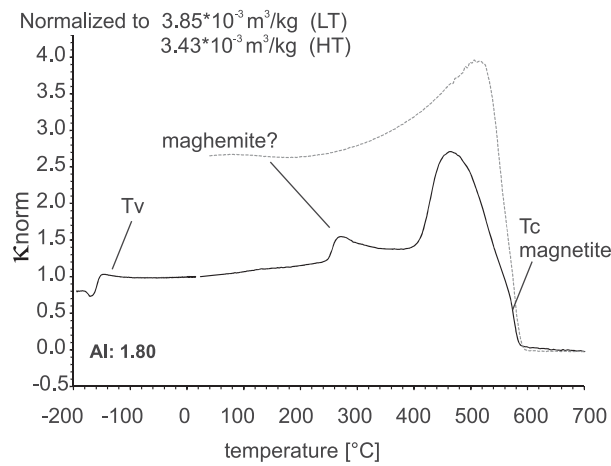
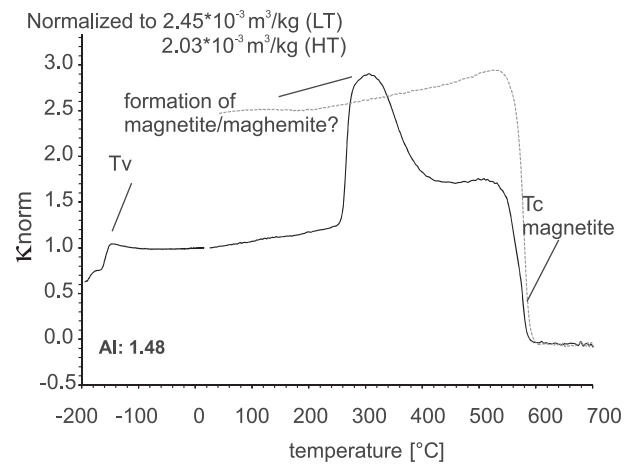
to fault zones with an intense brittle deformation and brecciation of the granite as well as alteration halos in the adjacent wall rocks. Illite along with Fe-carbonates, pyrite and hematite (martite) occur as alteration minerals, which are shown to transform into ferrimagnetic magnetite during heating in κ - T curves and, therefore, can be recognized easily. The strong irreversibility of κ - T curves for the highly altered stage II samples observed by Just & Kontny (2012) was also seen in our κ - T measurements from the cuttings (Fig. 10a). The most important transformation seen in κ - T curves is the one from hematite into magnetite. In addition, we found Fe-bearing carbonates in the cuttings, which are observed in the κ - T curves by the transformation into magnetite above 400 °C. In addition to these mineral transformations, we recognized in nearly all samples another phase with a peak in susceptibility at about 300 °C, which is not described from the EPS1 core material. This phase is most likely related to the oxidation products of iron flakes, which occur as contamination in the cuttings and could also be seen in κ - T curves of iron chips separated from the cuttings. The peak might reflect the formation of maghemite from oxidation products of the iron contaminants during heating of the samples (Taylor & Schwertmann 1974; Gendler *et al.* 2005).

Iron flakes have been observed microscopically (Fig. 9a) and in some κ - T curves (Fig. 10c). Especially in the cuttings from the longest stored GPK1, these iron flakes are strongly oxidized to a mixture of different Fe-oxides. Due to the lower content of fresh iron in GPK1 cuttings, the GPK1 sample portion separated for κ - T measurements might be free of original iron flakes and just contain the oxidation products. Therefore, GPK1 magnetic susceptibility decreases to paramagnetic values above 600 °C, while still showing the peak below 300 °C. The contamination of the cuttings by iron flakes can significantly disturb the correlation between magnetic susceptibility and SCCL. For example, GPK1-C40 (3485 m, see Fig. 5b) from the altered granite shows a higher magnetic susceptibility than we might expect according to its alteration degree (Fe-bearing carbonates, high amount of hematite, few magnetite). Therefore, the iron contamination must be eliminated before magnetic susceptibility measurements, which was not done in this study.

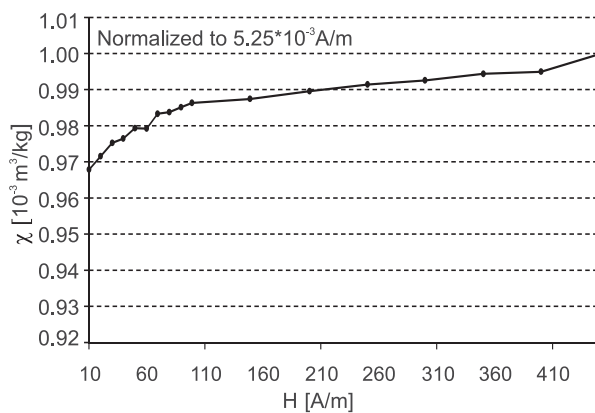
Our study has shown that high χ in combination with low alteration index ($AI < 1$) is typical for the porphyritic granite and low χ in combination with negative alteration index ($AI < 0$) is typical for the two-mica granite. Low magnetic susceptibility in combination with strongly irreversible κ - T curves ($AI > 1$) and the formation of magnetite above 400 °C clearly indicates alteration stage II, which has also produced the highest amount of clay minerals. There are several reasons for high magnetic susceptibility, which we identified by microscopic investigations. High magnetic susceptibility is either related to a high amount of fresh magnetite in unaltered rock or due to secondary formation of magnetite in extremely altered samples. Furthermore, high χ can be caused by contaminations with iron debris from the drilling tools. Low χ is a result of magnetite oxidation in the course of hydrothermal alteration, but it can also be attributed to a primary low magnetite proportion in cutting material. The latter effect explains why also fresh, unaltered granite have low χ (Fig. 6).

7.3 Calibration of SCCLs

Magnetic susceptibility measurements from the EPS1 core and clay concentration calculated from borehole measurements (SCCL) show a strong correlation (Fig. 2) suggesting that magnetic

(a) κ -T curve: GPK1-C40; 3497m(c) κ -T curve: GPK1-C73; 3536m

(b) GPK1-C40; 3497m



(d) GPK1-C73; 3536m

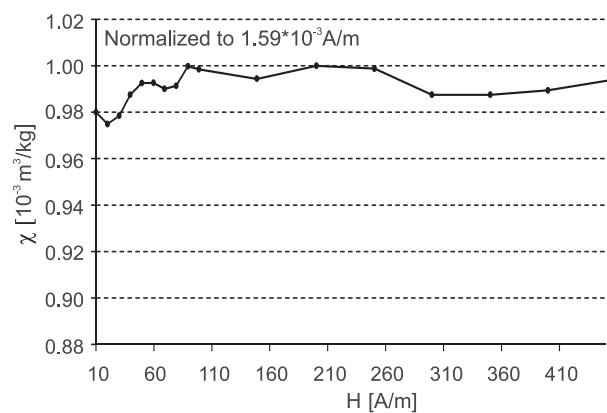


Figure 12. κ -T curves and field dependency of the samples GPK1-C40 and GPK1-C73. The κ -T curves (a and c) show the formation of several mineral phases during the heating run. The formation of pyrrhotite can be excluded, as the samples show no field dependency (b and d).

susceptibility can be used in the magnetite-bearing Soultz granite as an independent alteration indicator. One of the goals of this study was to investigate the applicability of magnetic susceptibility measurements on cuttings as a calibration tool for the SCCL logs of the deep wells GPK1-4. We found magnetite as the primary magnetic mineral in all samples independent of their facies. The degree of magnetite oxidation to hematite indicates rock alteration and thus the presence of clay minerals. In several depth intervals, SCCL and χ were inversely correlated, but we could identify several difficulties. In general, we found a reasonable correlation between the different SCCL groups and magnetic susceptibility of cuttings (Fig. 6), although there is a large scattering of magnetic susceptibility values, especially in the fresh granite. The reason for this large scattering is probably a mixture of rock chips from certain depth intervals and the inhomogeneous distribution of magnetite within the granite. The larger the sampling interval, the more different granite types (porphyritic versus two-mica granite and fresh versus altered granite) can be mixed and the resolution and quality of χ measurements is hampered. Petrographic changes smaller than few meters thickness cannot be seen. Some small rock pieces might also get lost during their vertical transport uphole and clay minerals may be dissolved. Furthermore, there can be enrichment in flaky minerals like biotite and muscovite. Due to their shape, they float on the mud, as it has for example been observed in GPK4 (Dezayes *et al.* 2005), where biotite was enriched. Washing of the cuttings of

GPK3 and GPK4 could also have affected the mineralogical content by dissolving small particles.

In terms of calibration of the SCCL we can state that it is not straightforward postulating high clay content for low χ samples and no clay in high χ samples respectively, but the analysis showed that high magnetic susceptibility is only systematically measured in fresh samples. It is possible to calibrate the SCCL at least for intervals, where no clay is expected. For the remaining intervals, susceptibility of cuttings can be used as an auxiliary means to calibrate the SCCL log.

8 CONCLUSION

In this study, we introduced a new method to identify altered and clay-rich zones within a magnetite-bearing granitic reservoir. For the first time, SCCL have been created from borehole logs by a neural network analysis indicating the alteration along the deep wells in Soultz-sous-Forêts. These logs can be interpreted on the basis of magnetic mineralogical investigations of cuttings, describing the mineral transformations resulting from hydrothermal alteration in the deeper part of the granitic reservoir.

Magnetic susceptibility measurements on cuttings allow a calibration of SCCL logs. By comparing EPS1 core and GPK1-4 cuttings magnetic susceptibility data with the calculated SCCL,

we were able to define intervals with fresh and altered granite albeit with different success. This study, however, revealed that petrographic investigations in combination with κ - T curves on cuttings material are powerful tools to decipher different granite types and different degrees of alteration. The degree of alteration is reflected by χ , which is lower for highly altered samples. Low χ can also be observed in fresh granite types with a primary low magnetite proportion, but can be discriminated by magnetic mineralogical investigations.

For a better resolution of the data and for calibration measurements, we suggest a sampling interval for the cuttings of ideally 1 m. Furthermore, iron contaminations from the drill bit should be eliminated prior to magnetic mineralogical investigations in order to receive better results.

Being so far merely a by-product of drilling and only used for creating lithology logs and chemical analysis, cuttings should be paid more attention for reservoir characterization, as they provide significant information. Magnetic susceptibility of the cuttings is fast and easily measured. In order to be able to correctly interpret the measuring results, petrographic investigations like transmitted and reflected light microscopy of thin sections, REM, EDX and κ - T measurements are necessary. With these methods, the magnetic mineral assemblage can be identified and the alteration processes can be reconstructed.

Based on the results of this study, further investigations on fracture mechanics and hydraulics related to the appearance of clay inside fractures are made possible. The effect of clay inside fractures on induced seismicity is one of the major issues to be investigated. Furthermore, the influence of clay on fracture permeability needs to be further analysed and will be the topic of future work.

ACKNOWLEDGEMENTS

This research was conducted within the portfolio topic GEOENERGIE of the Helmholtz Association of German Research Centers and was funded by Energie Baden-Wuerttemberg (EnBW), Germany. The authors are grateful to GEIE Exploitation minière de la chaleur for providing the Soultz borehole data and to the French geological survey (BRGM) in Orléans, who provided us the cutting material, especially to Chrystel Dezayes, who made the effort to track the desired intervals out. Thin sections have been prepared by Stephan Unrein and Kristian Nikoloski. The work on the REM and EDX was made possible by the friendly support of Volker Zibat from the laboratory of electron microscopy (LEM) at KIT in Karlsruhe. Finally, we are grateful to the reviewers who contributed to an improvement of the quality of this manuscript.

REFERENCES

- Angerer, T., Greiling, R.O. & Avigad, D., 2011. Fabric development in a weathering profile at a basement–cover interface, the sub-Cambrian penepplain, Israel: implications for decollement tectonics, *J. Struct. Geol.*, **33**, 819–832.
- Baisch, S., Voros, R., Rothert, E., Stang, H., Jung, R. & Schellschmidt, R., 2010. A numerical model for fluid injection induced seismicity at Soultz-sous-Forêts, *Int. J. Rock Mech. Mining Sci.*, **47**, 405–413.
- Catalli, F., Meier, M.A. & Wiemer, S., 2013. The role of Coulomb stress changes for injection-induced seismicity: the Basel enhanced geothermal system, *Geophys. Res. Lett.*, **40**, 72–77.
- Cornell, R.M. & Schwertmann, U., 2003. *The Iron Oxides: Structure, Properties, Reactions, Occurrences and Uses*, 2nd edn, Wiley-VCH, pp. 703.
- Dezayes, C., Chèvremont, P., Tourlière, B., Homeier, G. & Genter, A., 2005. Geological study of the GPK4 HFR borehole and correlation with the GPK3 borehole (Soultz-sous-Forêts, France), Open File Report, BRGM, OR, pp. 94.
- Dezayes, C., Genter, A., Homeier, G., Degouy, M. & Stein, G., 2003. Geological study of GPK3 HFR borehole (Soultz-sous-Forêts, France), Open File Report, BRGM, OR, pp. 128.
- Dezayes, C., Valley, B., Maqua, E., Syren, G. & Genter, A., 2000. Natural fracture system of the Soultz granite based on UBI Data in the GPK3 and GPK4 Wells, Synthetic final report, BRGM, pp. 11.
- Dunlop, D.J. & Özdemir, Ö., 1997. *Rock Magnetism*, 1st edn, Cambridge Univ. Press, pp. 595.
- Edel, J.B., Schulmann, K., Skrzypek, E. & Cocherie, A., 2013. Tectonic evolution of the European Variscan belt constrained by palaeomagnetic, structural and anisotropy of magnetic susceptibility data from the Northern Vosges magmatic arc (eastern France), *J. Geol. Soc.*, **170**, 785–804.
- Fritz, B., Jacquot, E., Jacquemont, B., Baldeyrou-Bailly, A., Rosener, M. & Vidal, O., 2010. Geochemical modelling of fluid-rock interactions in the context of the Soultz-sous-Forêts geothermal system, *Cr. Geosci.*, **342**, 653–667.
- Gendler, T.S., Shcherbakov, V.P., Dekkers, M.J., Gapeev, A.K., Gribov, S.K. & McClelland, E., 2005. The lepidocrocite–maghemite–haematite reaction chain—I. Acquisition of chemical remanent magnetization by maghemite, its magnetic properties and thermal stability, *Geophys. J. Int.*, **160**, 815–832.
- Genter, A. & Traineau, H., 1992. Hydrothermally altered and fractured granite as an HDR reservoir in the EPS-1 borehole, Alsace, France, in *Proceedings of the Seventeenth Workshop on Geothermal Reservoir Engineering*, Stanford University, Stanford, California, SGP-TR-141, 6.
- Genter, A. & Traineau, H., 1993. Deepening of GPK-1 HDR borehole 2000–3600m (Soultz-sous-Forêts, France), Geological Monitoring, Report BRGM, BRGM-IMRG, BRGM, Orléans, pp. 25.
- Genter, A. & Traineau, H., 1995. Fracture analysis in Granite in the HDR Geothermal EPS-1 Well, Soultz-Sous-Forêts, France, BRGM Rapport, 53.
- Guillou-Frottier, L., Carre, C., Bourguin, B., Bouchot, V. & Genter, A., 2013. Structure of hydrothermal convection in the Upper Rhine Graben as inferred from corrected temperature data and basin-scale numerical models, *J. Volc. Geotherm. Res.*, **256**, 29–49.
- Hooijkaas, G.R., Genter, A. & Dezayes, C., 2006. Deep-seated geology of the granite intrusions at the Soultz EGS site based on data from 5 km-deep boreholes, *Geothermics*, **35**, 484–506.
- Hrouda, F., 2003. Indices for numerical characterization of the alteration processes of magnetic minerals taking place during investigation of temperature variation of magnetic susceptibility, *Stud. Geophys. Geod.*, **47**, 847–861.
- Ishihara, S., 1977. The magnetite-series and Ilmenite-series granitic rocks, *Min. Geol.*, **27**, 293–305.
- Just, J., 2005. Modification of magnetic properties in granite during hydrothermal alteration (EPS-1 borehole, Upper Rhine Graben), *PhD thesis*, University of Heidelberg, Heidelberg.
- Just, J. & Kontny, A., 2012. Thermally induced alterations of minerals during measurements of the temperature dependence of magnetic susceptibility: a case study from the hydrothermally altered Soultz-sous-Forêts granite, France, *Int. J. Earth Sci. (Geol. Rundsch.)*, **101**, 819–839.
- Just, J., Kontny, A., De Wall, H., Hirt, A.M. & Martín-Hernández, F., 2004. Development of magnetic fabrics during hydrothermal alteration in the Soultz-sous-Forêts granite from the EPS-1 borehole, Upper Rhine Graben, *Geol. Soci., Lond. Spec. Publ.*, **238**, 509–526.
- Kohonen, T., 1984. *Self-Organization and Associative Memory*, 1st edn, Springer, pp. 255.
- Kontny, A., de Wall, H., Sharp, T.G. & Pósfai, M., 2000. Mineralogy and magnetic behavior of pyrrhotite from a 260 °C section at the KTB drilling site, Germany, *Am. Miner.*, **85**, 1416–1427.
- Lagoeiro, L.E., 1998. Transformation of magnetite to hematite and its influence on the dissolution of iron oxide minerals, *J. Metamorph. Geol.*, **16**, 415–423.

- Ledéserf, B., Joffre, J., Amblès, A., Sardini, P., Genter, A. & Meunier, A., 1996. Organic matter in the Soultz HDR granitic thermal exchanger (France): natural tracer of fluid circulations between the basement and its sedimentary cover, *J. Volc. Geotherm. Res.*, **70**, 235–253.
- Meller, C., Genter, A. & Kohl, T., 2014. The application of a neural network to map clay zones in crystalline rock, *Geophys. J. Int.*, **196**, 837–849.
- Moore, D.E. & Lockner, D.A., 2013. Chemical controls on fault behavior: weakening of serpentinite sheared against quartz-bearing rocks and its significance for fault creep in the San Andreas system, *J. geophys. Res.: Solid Earth*, **118**, 2558–2570.
- Oliva-Urcia, B., Kontny, A., Vahle, C. & Schleicher, A.M., 2011. Modification of the magnetic mineralogy in basalts due to fluid–rock interactions in a high-temperature geothermal system (Krafla, Iceland), *Geophys. J. Int.*, **186**, 155–174.
- Pandarinath, K., Shankar, R., Torres-Alvarado, I. & Warriar, A., 2013. Magnetic susceptibility of volcanic rocks in geothermal areas: application potential in geothermal exploration studies for identification of rocks and zones of hydrothermal alteration, *Arab J. Geosci.*, **7**(7), 2857–2860.
- Petronis, M.S., O’Driscoll, B. & Lindline, J., 2011. Late stage oxide growth associated with hydrothermal alteration of the Western Granite, Isle of Rum, NW Scotland, *Geochem., Geophys., Geosyst.*, **12**, Q01001, doi:10.1029/2010GC003246.
- Rummel, F. & König, E., 1991. Physical properties of core samples borehole EPS1 Soultz-sous-Forêts, velocity-, density- and magnetic susceptibility-logs, depth interval 933-2227m, Yellow Reports, Ruhr-University, Bochum, pp. 58.
- Rummel, F., König, E. & Rybacki, E., 1991. Physical properties of core samples borehole EPS1 Soultz-sous-Forêts, velocity-, density- and magnetic susceptibility-logs, depth interval 1410-1980m, Yellow Reports, Ruhr-University, Bochum, pp. 35.
- Rummel, F. & Schreiber, D., 1993. Physical properties of the core K21 borehole GPK1 Soultz-sous-Forêts depth interval 3522.58-3525.88m, Yellow Reports, Ruhr-University, Bochum, pp. 11.
- Schleicher, A.M., 2005. Clay mineral formation and fluid-rock interaction in fractured crystalline rocks of the Rhine rift system: case studies from the Soultz-sous-Forêts granite (France) and the Schauenburg Fault (Germany), *Dipl.-Geol. Inaugural Dissertation*, Ruprecht-Karls-Universität, Heidelberg.
- Tauxe, L., 1998. *Paleomagnetic Principles and Practice*, 1st edn, Springer, pp. 301.
- Taylor, R.M. & Schwertmann, U., 1974. Maghemite in soils and its origin—II. Maghemite syntheses at ambient temperature and pH7, *Clay Miner.*, **10**, 299–310.
- Valley, B. & Evans, K., 2003. Strength and elastic properties of the Soultz Granite, *Synthetic 2nd year report 6*, Zürich, Switzerland.